

# Abundance of the Multiheme $c$ -Type Cytochrome OmcB Increases in Outer Biofilm Layers of Electrode-Grown *Geobacter sulfurreducens*

Camille S. Stephen<sup>1</sup>, Edward V. LaBelle<sup>2</sup>, Susan L. Brantley<sup>3</sup>, Daniel R. Bond<sup>2,4\*</sup>

**1** Department of Biochemistry and Molecular Biology, The Pennsylvania State University, University Park, Pennsylvania, United States of America, **2** BioTechnology Institute, University of Minnesota, St. Paul, Minnesota, United States of America, **3** Department of Geosciences, The Pennsylvania State University, University Park, Pennsylvania, United States of America, **4** Department of Microbiology, University of Minnesota, St. Paul, Minnesota, United States of America

## Abstract

When *Geobacter sulfurreducens* utilizes an electrode as its electron acceptor, cells embed themselves in a conductive biofilm tens of microns thick. While environmental conditions such as pH or redox potential have been shown to change close to the electrode, less is known about the response of *G. sulfurreducens* to growth in this biofilm environment. To investigate whether respiratory protein abundance varies with distance from the electrode, antibodies against an outer membrane multiheme cytochrome (OmcB) and cytoplasmic acetate kinase (AckA) were used to determine protein localization in slices spanning  $\sim 25$   $\mu\text{m}$ -thick *G. sulfurreducens* biofilms growing on polished electrodes poised at +0.24 V (vs. Standard Hydrogen Electrode). Slices were immunogold labeled post-fixing, imaged via transmission electron microscopy, and digitally reassembled to create continuous images allowing subcellular location and abundance per cell to be quantified across an entire biofilm. OmcB was predominantly localized on cell membranes, and 3.6-fold more OmcB was detected on cells 10–20  $\mu\text{m}$  distant from the electrode surface compared to inner layers (0–10  $\mu\text{m}$ ). In contrast, acetate kinase remained constant throughout the biofilm, and was always associated with the cell interior. This method for detecting proteins in intact conductive biofilms supports a model where the utilization of redox proteins changes with depth.

**Citation:** Stephen CS, LaBelle EV, Brantley SL, Bond DR (2014) Abundance of the Multiheme  $c$ -Type Cytochrome OmcB Increases in Outer Biofilm Layers of Electrode-Grown *Geobacter sulfurreducens*. PLoS ONE 9(8): e104336. doi:10.1371/journal.pone.0104336

**Editor:** Hauke Smidt, Wageningen University, Netherlands

**Received:** March 21, 2014; **Accepted:** July 14, 2014; **Published:** August 4, 2014

**Copyright:** © 2014 Stephen et al. This is an open-access article distributed under the terms of the Creative Commons Attribution License, which permits unrestricted use, distribution, and reproduction in any medium, provided the original author and source are credited.

**Data Availability:** The authors confirm that all data underlying the findings are fully available without restriction. All relevant data are within the paper and its Supporting Information files.

**Funding:** This work was supported by the following funding sources: the National Science Foundation, which funded The Center for Environmental Kinetics Analysis under Grant No. CHE-0431328 (S.L.B., C.S.S.) ([www.nsf.gov](http://www.nsf.gov)); Alfred P. Sloan Foundation Graduate Scholarship program (C.S.S.) (<http://sloanphds.org/sloan/Sloan.aspx?pageid=30>); U.S. Department of Energy under Grant No. DE-SC0007058 (M.T.) (<http://energy.gov/>); The Office of Naval Research under Grant No. N000140810162 (E.V.L.) ([www.onr.navy.mil](http://www.onr.navy.mil)); and U.S. Department of Energy, Office of Science (Biological and Environmental Research) under Grant No. DE-SC0006868 (D.R.B.) (<http://science.energy.gov/ber/>). The funders had no role in study design, data collection and analysis, decision to publish, or preparation of the manuscript.

**Competing Interests:** The authors have declared that no competing interests exist.

\* Email: [dbond@umn.edu](mailto:dbond@umn.edu)

## Introduction

The anaerobic respiratory strategy known as dissimilatory metal reduction likely evolved long before the Earth's atmosphere became aerobic [1,2], and remains a significant process for geochemical cycling in sediments and subsurface environments [1,3]. As reduction of metal oxides can support microbial oxidation of organic contaminants, and microbial reduction can alter the solubility of metals, dissimilatory metal reduction is also of involved in bioremediation and bioprecipitation of heavy metals [4–6]. A model metal-reducing bacterium capable of reducing both soluble and insoluble metals is *Geobacter sulfurreducens* [7]. Like most *Geobacter* strains, *G. sulfurreducens* can also use electrode surfaces as terminal electron acceptors, allowing generation of electricity [8–10].

When in contact with electrodes, *G. sulfurreducens* cells are capable of electron transfer from cell membranes to support growth. Daughter cells then grow as layers upon each other, connected by pathways conductive enough to transfer electrons tens of microns, allowing respiration by all cells in the biofilm

[8,11,12]. Electron transfer by *G. sulfurreducens* electrode biofilms is dependent upon multiple extracellular proteins attached to cells [8,9,11], in contrast to representatives of the genus *Shewanella*, which rely on secreted FMN as a soluble electron shuttle for reduction of distant acceptors [8,13–16].

Within *Geobacter* electrode biofilms, nutrient, pH, redox or electrical gradients may exist that affect cell physiology. For example, conduction of electrons through active biofilms appears to become limiting at distances 10–20  $\mu\text{m}$  from the electrode surface, based on microelectrode [17], spectral [18,19], source-drain experiments [12,20], and confocal Raman spectroscopy [21]. A pH gradient can also exist across the biofilm, where the inner layers experience a lower pH [22–24].

The existence of these gradients has led to studies attempting to detect changes in gene expression across this narrow  $\sim 20$   $\mu\text{m}$  window between the electrode surface and outer layers. Franks et al. [25] performed the first microarray analysis on *G. sulfurreducens* biofilm layers by microtoming sections into inner (0–20  $\mu\text{m}$ ) and outer (30–60  $\mu\text{m}$ ) leaflets. Of 146 genes differentially

expressed [25] few differences were observed with genes linked to electron transfer, such as those encoding multiheme cytochromes, as well as subunits of Type IV pili. Immunogold labeling of the *G. sulfurreducens* extracellular cytochrome OmcZ suggested increased protein abundance close to the electrode ( $<5\ \mu\text{m}$ ) [26], but promoter fusion experiments visualizing *omcZ* expression were unable to detect any such gradient in *omcZ* expression, suggesting that differences in OmcZ could be due to mobility of this loosely attached cytochrome, or differences in cell density near the electrode [27].

For this work, a multiheme outer membrane cytochrome (OmcB) known to be regulated in response to environmental conditions [28–31] was selected as a target for an antibody-based approach for measuring changes in protein abundance within *Geobacter* anode biofilms. Acetate kinase was selected as a control for intracellular proteins. All measurements were performed using biofilms grown on polished anodes, to minimize variability in distance from the electrodes, and multiple high-resolution images were digitally reconstructed to obtain composite images spanning the entire biofilm for each labeling experiment. These data confirmed that direct labeling of resin-embedded *Geobacter* biofilms can be used to determine protein localization and detect changes in protein abundance throughout a biofilm.

## Results

### Biofilm growth

*G. sulfurreducens* cells attached to poised electrodes ( $n = 8$ ) with no lag, increased to a current density of  $>700\ \mu\text{A}/\text{cm}^2$ , and were all harvested at the same stage of growth (Fig. 1A). These growth rates and current densities were typical of *Geobacter* biofilms grown on polished graphite electrodes [8,11,32]. No biofilms demonstrated loss in current production when spent medium was removed and replaced with fresh medium. Cyclic voltammetry analysis yielded a sigmoidal catalytic wave with a characteristic midpoint potential (ca.  $-0.15\ \text{V}$ ) seen in growing *Geobacter* biofilms (Fig. 1B). Confocal microscopy of electrodes on which *G. sulfurreducens* biofilms were grown under similar conditions revealed biofilms of intact cells, based on Live/Dead staining, extending  $\sim 20\ \mu\text{m}$  from the electrode surface [8,33,34]. This thickness matched the resin-embedded slices imaged via TEM, indicating little shrinkage, collapse, or loss of the biofilm occurred during fixation.

Fig. 2A shows a representative TEM micrograph of a *G. sulfurreducens* biofilm grown on the anodic electrode, spanning over  $20\ \mu\text{m}$  (the electrode is indicated by the arrow). The cells growing closer to the electrode were longitudinally oriented, and densely packed, causing the cell density near the electrode to be over 30% higher than in regions more distant from the electrode.

### Analysis of OmcB abundance in biofilms using immunogold labeling

After development of anti-OmcB antibodies and labeling conditions (see Methods), 70-nm thick biofilm slices were immunogold labeled and imaged via TEM. Two trends were immediately apparent in all images and were later substantiated by quantitative analysis. First, the majority of OmcB labeling was associated with the cell membrane, indicating that proteins embedded in membranes were exposed by microtome slicing. Second, cells farther from the electrode ( $10\ \mu\text{m}$  to  $20\ \mu\text{m}$ ) had a higher density of membrane-associated OmcB. Representative images are shown in Fig. 2B and 2C. Particles counted as membrane-associated (within 15 nm of a visible membrane) are indicated in red, and intracellular particles are highlighted in

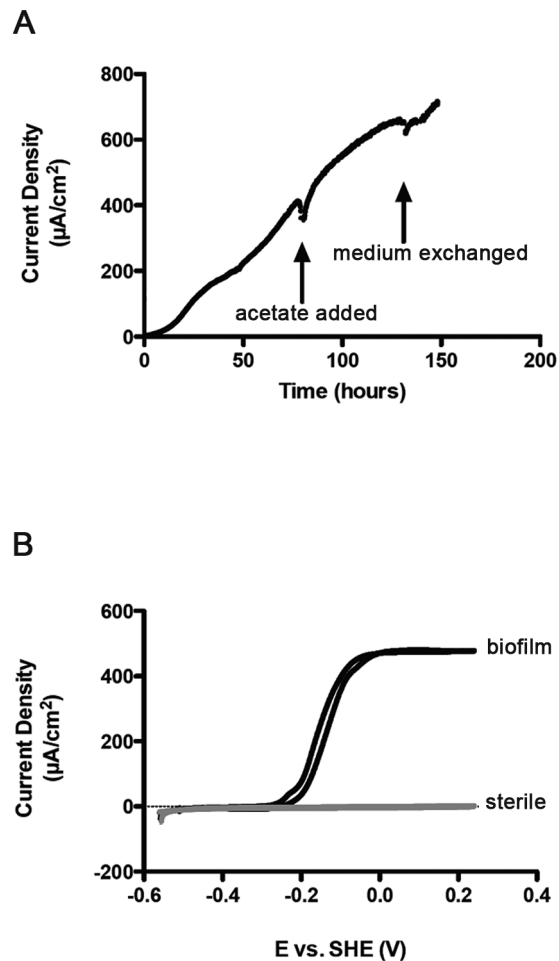


**Figure 1. Growth of biofilms for analysis.** (A) Representative trace showing current production by a *G. sulfurreducens* biofilm using 30 mM acetate as the electron donor on a polished graphite electrode poised at +0.24 V vs. Standard Hydrogen Electrode. Additional acetate (30 mM) was added where indicated, and the medium was replaced to remove planktonic cells. (B) Cyclic voltammetry (1 mV/s) of the electrode shown in A, producing the characteristic sigmoidal current response of a *G. sulfurreducens* biofilm-colonized electrode. All biofilms were grown simultaneously from the same inoculum under identical conditions, were harvested and fixed in resin at the same time. doi:10.1371/journal.pone.0104336.g001

black. The distance of 15 nm for membrane association was based on the length of the rabbit IgG antibody (8.6 nm), plus the length of secondary antibodies [35].

To better quantify the abundance and localization of OmcB, a series of 12–15 high-resolution TEM images at 10,000 $\times$  magnification were collected, and digitally re-assembled to produce a continuous picture of an entire biofilm. Each biofilm could then be divided into  $2\ \mu\text{m}$  sections, beginning from the electrode surface. Within each section, gold particles were separated into two categories; those inside the cell, and those at the membrane. A raw image showing the process of digital re-assembly using 13 high-resolution images is provided in Supplementary Information (Fig. S1). This sequence of slicing, high-resolution imaging, digital reconstruction, and abundance measurement was performed independently at least 3 times for OmcB quantification analyses.

Because cell density in the biofilm decreased away from the electrode, the number of gold particles had to be normalized for

A

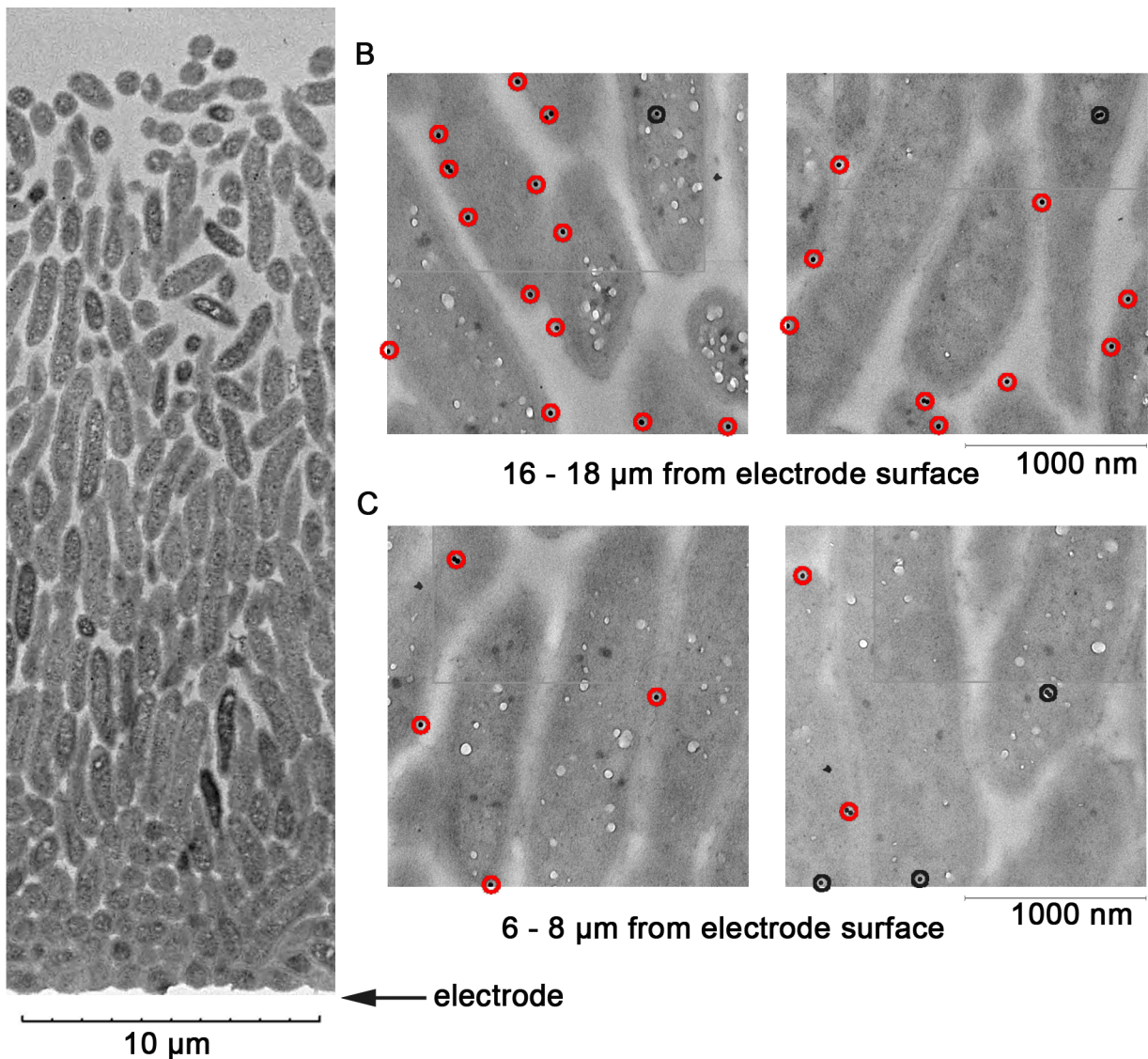


**Figure 2. Representative biofilm and labeling with anti-OmcB antibody.** (A) Low-resolution Transmission Electron Microscopy image showing an entire unlabeled *G. sulfurreducens* biofilm, illustrating increase in cell density near the electrode surface. (B) Examples from digitally reconstructed high-resolution images representing cells 16–18 μm from the electrode labeled with anti-OmcB antibodies. Red circles indicate proteins within 15 nm of the membrane, black circles indicate intracellular localization. (C) Examples of cells located 6–8 μm from the electrode, taken from the same biofilm reconstructions, with lower abundance of OmcB. doi:10.1371/journal.pone.0104336.g002

cell area present. Thus, the total abundance of OmcB (as total number of gold particles per  $\mu\text{m}^2$  of cells) could be expressed as a function of distance from the electrode and is shown in Fig. 3.

While some OmcB was always detected inside cells, presumably from apoproteins awaiting secretion, this baseline of intracellular OmcB labeling remained low throughout the biofilm (ca. 0.5 particles per  $\mu\text{m}^2$ ), with over 70% of the detected OmcB protein localized to the membrane in outer biofilm slices. However, the overall abundance of outer membrane-localized OmcB increased significantly with distance from the electrode. A range of 0.17 to 1.00 particles per  $\mu\text{m}^2$  was observed on cell membranes in the inner 10 μm of the biofilm, while a range of 2.15 to 3.42 particles per  $\mu\text{m}^2$  was observed on cell membranes in the outer 12–20 μm of the biofilm ( $n = 3$ ).

Statistical analysis (ANOVA with two factor replication) of OmcB abundance in slices close to the electrode vs. outer leaflets, as well as in the membrane vs. inside the cells, was performed to verify these differences. For all biofilms analyzed, the increase in OmcB labeling of cells 12–20 μm away from the electrode was significant at  $p$ -values  $< 0.001$ . The increased abundance of membrane vs. cytoplasmic labeling were significant at  $p < 0.03$  for all slices analyzed.

When the same labeling experiment was performed on slices using pre-immune serum, few particles were detected, and no trends in localization or abundance were observed. As this pre-immune serum was obtained from the same animals before exposure to the OmcB protein, and should not contain antibodies

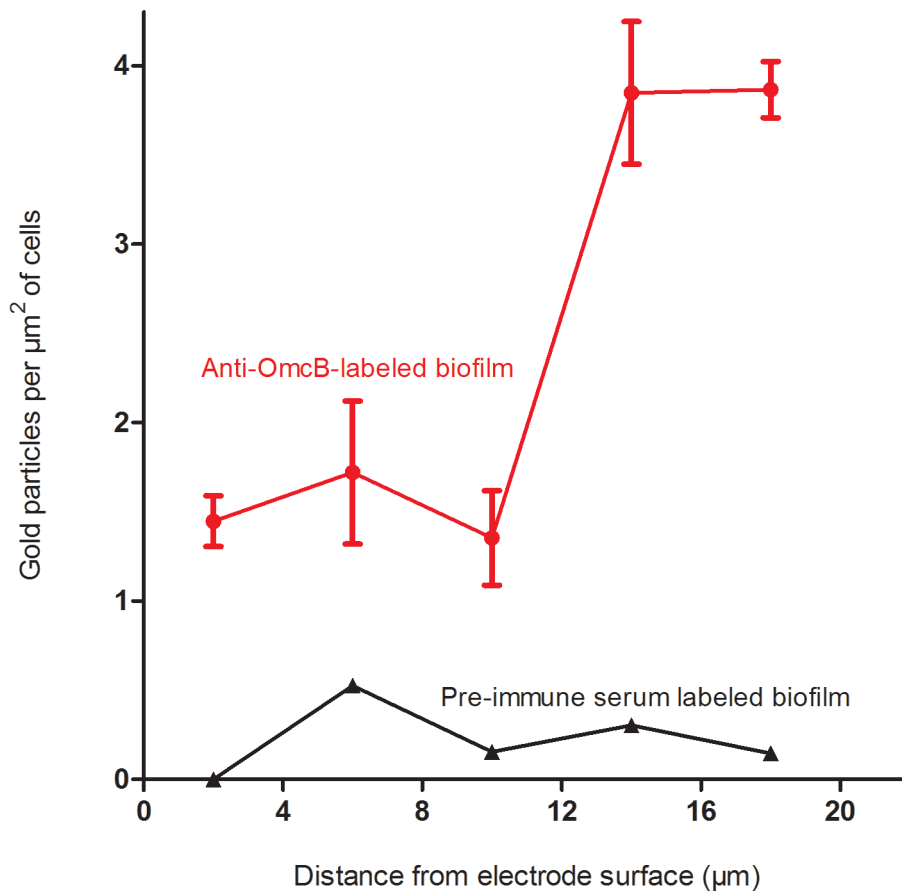


**Figure 3. Abundance of OmcB on *G. sulfurreducens* cells at different distances from the electrode.** Means shown are the result of six different images compiled from three different biofilms,  $\pm$  SEM. Data from labeling after incubation with *anti*-OmcB antibodies (red circles) vs. labeling with pre-immune serum as a control (black triangles). doi:10.1371/journal.pone.0104336.g003

to OmcB, this represented a control for non-specific labeling of *Geobacter* cells.

#### Analysis of acetate kinase immunogold labeling

Acetate kinase abundance was also analyzed by immunogold labeling, as a control for the ability to determine protein location, and as a marker for actively metabolizing cells. As with OmcB, multiple TEM images were assembled into contiguous sections from the electrode surface to the edge of the biofilm. Labeling inside cells was observed throughout the biofilm (Fig. 4A and 4B), and distance from the electrode had no effect on particle density. Cells 0–10  $\mu\text{m}$  away from the electrode contained a range of 2.33 to 2.92 particles per  $\mu\text{m}^2$  of cells, while sections farther from the electrode contained 1.68 to 2.68 particles per  $\mu\text{m}^2$  of cells. In all regions of the biofilm, 78% of particles were detected on the interior of the cells, with very rare instances of labeling between cells which could indicate cell lysis or release of acetate kinase. Nonspecific labeling was also low for the acetate kinase pre-immune serum labeled biofilm (Fig. 5).

#### Discussion

When *Geobacter* species oxidize acetate, they are absolutely dependent upon electron transfer to a terminal electron acceptor for energy generation. Compared to the use of metal oxide particles or soluble compounds, the electrode biofilm environment

creates unique physiological challenges [23,24,36,37]. In addition to the need to maintain a conductive network able to carry an ever-increasing burden when growing in cell layers more distance from the electrode, transfer of negatively charged electrons into the electrode creates a need for positive charge to diffuse outward to maintain both charge and pH balance [12,17,19,23]. Much recent research has been focused on how, or if, *Geobacter* responds to these challenges.

While many multiheme *c*-type cytochromes may play roles in metal reduction [28,38–43], one cytochrome that is conserved and consistently identified in studies with *G. sulfurreducens* is OmcB. OmcB is a putative lipoprotein dodecaheme *c*-type cytochrome which fractionates in the outer membrane fraction [44,45], and has been shown via immunolocalization to be exposed on the outer surface [46]. Many mutant phenotypes in Fe(III) reduction can be traced to defects in *omcB* expression or translation [40,47,48]. For example, deletion of the gene encoding the diheme peroxidase MacA decreases *omcB* transcripts to undetectable levels and negatively impacts Fe(III) reduction, while expression of *omcB* from a constitutive promoter in a  $\Delta\text{macA}$  mutant restores Fe(III) reduction [40,47,49–51]. As one of the most conserved cytochromes among the *Geobacteraceae*, and as the cytochrome most often linked to electron transfer beyond the cell membrane, OmcB was chosen as a target for this proof-of-concept study.

Changes in cytochrome expression by planktonic cells during Fe(III)- or electrode reduction have been reported using DNA

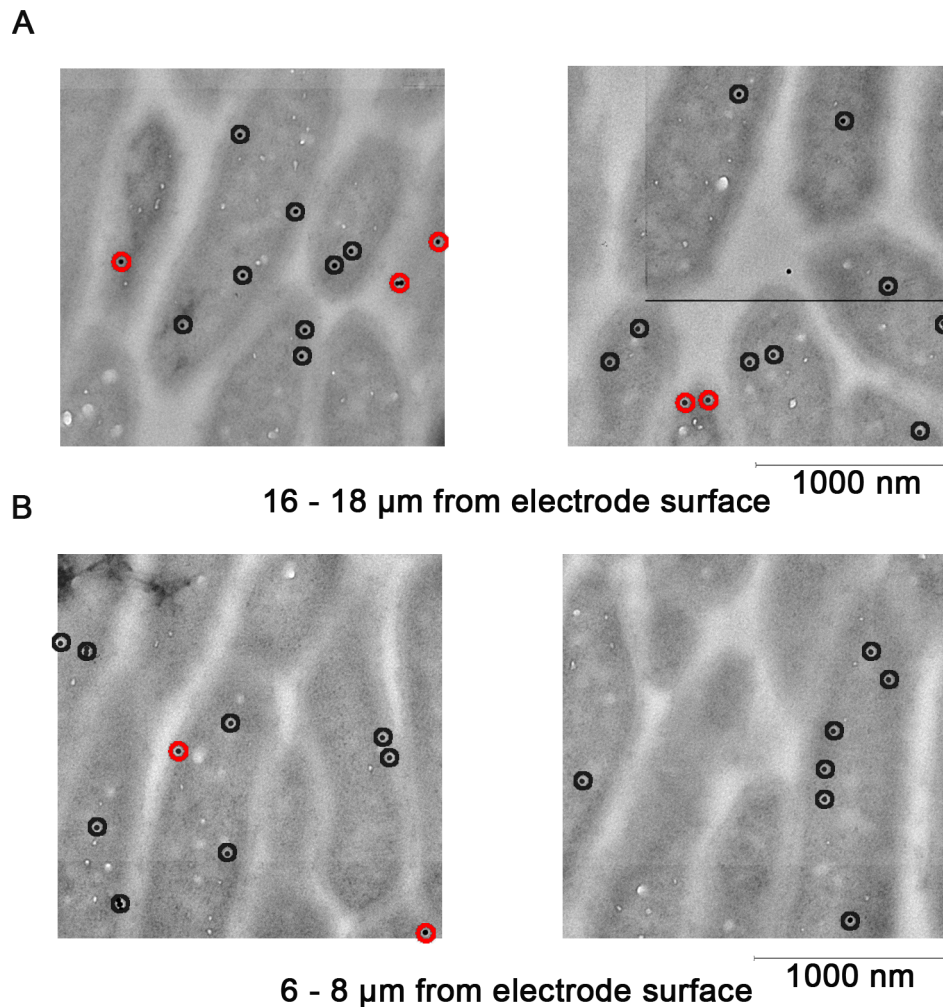


**Figure 4. Anti-Acetate kinase labeling of *G. sulfurreducens* biofilms.** (A) Examples from digitally reconstructed high-resolution images representing cells 16–18  $\mu\text{m}$  from the electrode labeled with *anti*-acetate kinase antibodies. Red circles indicate proteins within 15 nm of the membrane, black circles indicate intracellular localization. (B) Examples of cells located 6–8  $\mu\text{m}$  from the electrode, taken from the same biofilm reconstructions.

doi:10.1371/journal.pone.0104336.g004

microarray [52,53] and proteomic [31,42] approaches. However, as cells in a biofilm are not all exposed to identical conditions, such global analyses may represent averages that hide local microenvironments. We hypothesized that by assembling high-resolution images from biofilms growing on surfaces to minimize variability in cell age and distance from the electrode, while accounting for differences in cell density, quantitative data related to both cellular location and overall protein abundance per cell could be obtained.

In these experiments, the total abundance of OmcB was found to increase with distance from the electrode, a finding that could be due to two factors; differences in protein abundance per cell, or variability in antibody labeling. With regards to antibody labeling, thin resin-embedded cell sections are commonly used to quantify integral membrane proteins in different bacterial genera, even when cells are closely associated [53–57]. While methods that use flash-freezing can preserve delicate aspects of cellular ultrastructure, the antigenicity of target proteins is better preserved in resin-embedded samples, likely because freeze-substitution methods require use the chemical fixative osmium tetroxide, which affects protein antigenicity [55].

To minimize labeling artifacts in this study, slicing was used to give antigens equal probability of being exposed, compared to *in situ* labeling prior to slicing where cell packing or association limits access. Raw *G. sulfurreducens* images (provided in Fig. S1) demonstrated labeling at both cell-cell junctions and exposed membranes, providing supporting evidence that some antigens at the interface were accessible to antibodies, regardless of local conditions. While chosen for its reported lack of bias [58], the resin embedding-slicing method suffers from the fact that it must only label a very small percentage of proteins present in membranes, as each slice likely contains hundreds of OmcB targets, only a few of which are exposed at the interface. To compensate for this low efficiency, all embedding, slicing, and labeling steps were performed together, so that changes in the amount of detected protein could best reflect overall abundance.

If OmcB is more abundant in upper sections of the electrode-grown biofilm, then what could cells be responding to? Expression of *omcB* is affected by the stress-related sigma factor RpoS [59–61] and the stringent response [62,63]. More relevant to growth in these biofilms, which were under constant electron donor levels and nutrient conditions, is the fact that expression of *omcB*

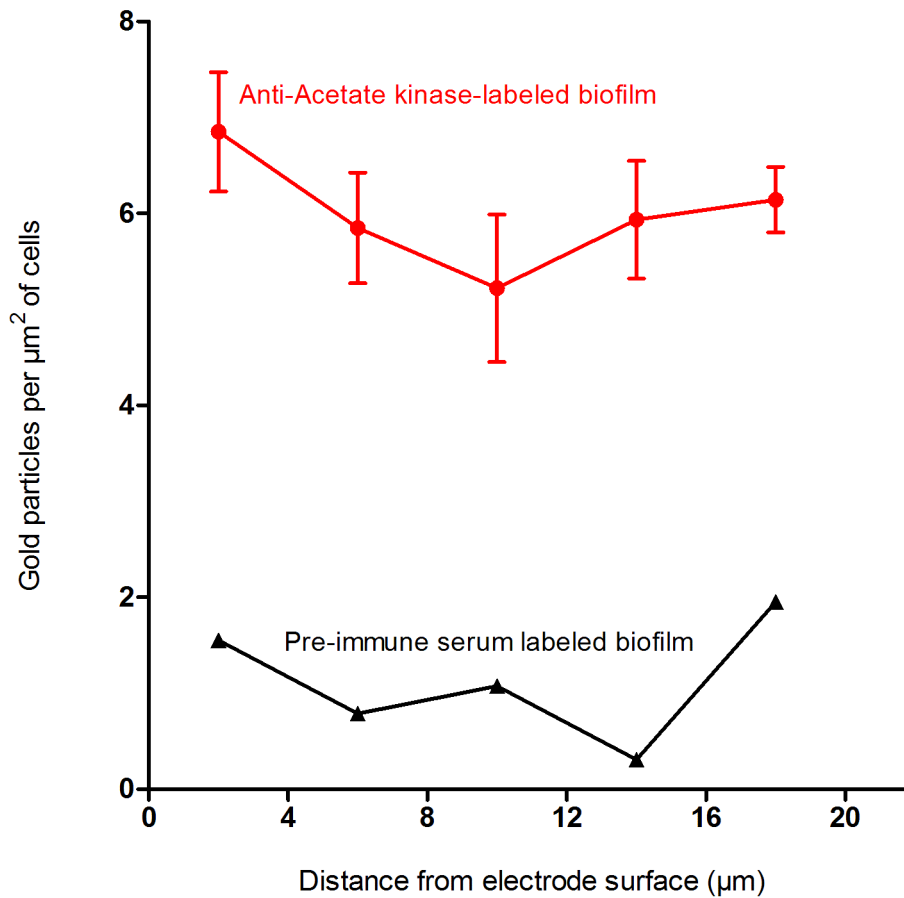


**Figure 5. Abundance of acetate kinase isozymes at different distances from the electrode.** Means shown are the result of six different images,  $\pm$  SEM. Data from labeling after incubation with *anti*-acetate kinase antibodies (red circles) vs. labeling with pre-immune serum as a control (black triangles).

doi:10.1371/journal.pone.0104336.g005

increases when *G. sulfurreducens* is limited for Fe(III) as an electron acceptor [30,64]. One hypothesis is that, as layers farther away from the electrode become more reduced, less electron acceptor is available in these regions, and OmcB increases in response. More generally, if the outer regions of the biofilm offer fewer opportunities for electron transfer, extra electron transfer machinery may be needed to achieve similar rates of electron disposal.

The concept that the outer portion of the *Geobacter* electrode biofilm represents a zone of electron acceptor limitation is not new. Spectral observations show nearly 50% of *c*-type cytochromes remain reduced when cells are growing in films similar to those used in this study [19], an observation also supported by confocal Raman spectroscopy [21]. Microelectrodes probing thicker ( $\sim 150 \mu\text{m}$ ) *G. sulfurreducens* biofilms growing on electrodes showed that outer regions of the biofilm were at low redox potential, and oxidized zones were only detected in the inner portion of the film [17]. Source-drain measurements using *G. sulfurreducens* films grown across small gaps also showed that redox potential can be significantly lower only 10  $\mu\text{m}$  away from an oxidizing electrode [12]. As OmcB appears to increase along the same spatial scales, this suggests that *Geobacter* can sense and respond to redox potential, in a manner similar to their known ability to sense Fe(III) availability.

In contrast to OmcB, acetate kinase labeling was consistent across the biofilm, providing no evidence for changes in acetate

concentrations. As these cells were cultivated with high levels of acetate (30 mM), and acetate is never depleted below saturating concentrations in these thin biofilms, the finding of consistent acetate kinase levels was not surprising. Redox stains and viability stains [25,27], have also provided evidence of active metabolism throughout biofilms of this thickness.

Overall, these results support use of immunogold labeling and biofilm reconstruction to simultaneously study both protein localization and abundance with high resolution. In this initial experiment, a difference in OmcB abundance was detected, and the protein was associated with cell surfaces even in biofilms where extensive extracellular connections are known to form. Experiments are needed that apply this approach to different growth conditions, such as changes in electrode redox potential. These experiments could also target proteins hypothesized to be secreted into the space between *Geobacter* cells, which offer opportunities for calibration against other *in situ* labeling methods, and provide a quantitative understanding of how the conductive matrix changes to support extracellular respiration in different regions of the biofilm.

## Experimental Procedures

### Bacterial growth conditions

*Geobacter sulfurreducens* PCA was routinely grown with Fe(III) oxide (100 mM) as the electron acceptor and 20 mM acetate as

the electron donor, and transferred 5 times into mineral media with 20 mM acetate and 40 mM fumarate when cells were needed for electrode growth [8]. All incubations were performed at 30°C under a 20% CO<sub>2</sub>/80% N<sub>2</sub> atmosphere. The bioreactor consisted of a jacketed glass electrochemical cell (Pine Instruments, Raleigh, NC) fitted with custom Teflon stoppers, sample ports and gas inlets. Working electrodes consisted of 2 cm<sup>2</sup> AXF-5Q graphitic carbon electrodes (Poco Graphite Company, Decatur, TX) that were polished with a 0.05 μm alumina slurry (BASi, West Lafayette, IN), sonicated in deionized water, and cleaned with acetone, 1 M NaOH, 1 M HCl, and rinsed with deionized water between each step. Eight graphite electrodes were suspended on 0.25 mm platinum wires (Sigma-Aldrich, St. Louis, MO) that were soldered to copper wire heat-sealed inside 3 mm glass capillary tubing (Kimble, Vineland, NJ). Counter electrodes of Pt were also constructed in this manner. A Vycor frit-tipped Luggin tube with a 0.1 M Na<sub>2</sub>SO<sub>4</sub> 1% agar salt bridge housed a calomel reference electrode (Cole-Parmer, Vernon Hills, IL). Electrodes were placed in stirred reactors, and connected to channels of a VMP potentiostat (Bio-Logic, Knoxville, TN).

Cells were cultivated in medium with excess electron donor until the optical density at 600 nm reached 0.6, and 60 mL was transferred into the autoclaved reactor containing 60 mL of mineral media with 30 mM acetate. The electrodes were poised at 0.24 V *versus* standard hydrogen electrode (SHE), and 30 mM additional acetate was added at 80 hours. Fresh medium with 30 mM acetate was added as current plateaued (131 hours) to remove planktonic and loosely attached cells. Cyclic voltammetry was performed at 1 mV/s from -0.56 to 0.24 V vs. SHE on sterile reactors, and at various time points during growth. The biofilm-bearing electrodes were harvested at 150 hours, gently rinsed in sterile media and fixed in a solution of 3% paraformaldehyde and 0.05% glutaraldehyde buffered with 0.05 M sodium phosphate at pH = 6.8.

### Preparation of biofilms for TEM

After fixation, the biofilms were embedded in L.R. White Resin and the resin was allowed to polymerize. The biofilms were sectioned at the Penn State Microscopy and Cytometry Facility (University Park, PA) into vertical sections, so that each slice spanned the entire biofilm. The 70 nm thick sections were floated onto copper grids (carbon coated) and permitted to dry before immunolabeling.

### Cloning and heterologous expression of OmcB

The full length *omcB* gene (2235 bp) was amplified via PCR from *G. sulfurreducens* PCA genomic DNA. The primers used for amplification were OmcB forward primer: (GCTAGCATGAGTAGAAAAGTAACAAAGTAT) and OmcB reverse primer: (CTCGAGCGGACGGGTCGT), the *NheI* and *XhoI* restriction enzymes sites are underlined, respectively. The gene was sub-cloned into pGEM T-easy vector (Promega) and DH5α competent cells. Colonies were selected on ampicillin, IPTG and X-Gal plates (AIX plates) incubated at 37°C and then inoculated into Luria-Bertani (LB) medium with 100 μg/mL ampicillin to be screened for the *omcB* gene. Plasmid DNA was isolated from each culture using Macherey-Nagel Nucleospin kit and digested with *NheI* and *XhoI* restriction enzymes. The *omcB* gene was gel extracted and ligated into the pET21a(+) expression plasmid (Novagen) to produce a His-tag fusion protein through heterologous expression in BL21 (DE3) pEC86 competent cells. The pEC86 plasmid [65] contains genes required for heme maturation and also confers chloramphenicol resistance.

The transformed cells were selected on solid LB medium (incubated at 37°C) containing 200 μg/mL ampicillin and 10 μg/mL chloramphenicol. Colonies were selected and inoculated into LB medium containing 100 μg/mL ampicillin and 35 μg/mL chloramphenicol antibiotics and grown overnight at 37°C. For screening of OmcB expression, 1 mL of the cells were used as an inoculum in 11 mL LB medium with 100 μg/mL ampicillin and 35 μg/mL chloramphenicol antibiotics and grown at 37°C. Protein expression was induced with 1 mM IPTG when the optical density of the cells reached 0.6 at 600 nm. Induced cells were grown for 3 hours with shaking at 37°C. Expression was visualized on SDS-PAGE gels stained with Coomassie R-250 stain. Cells containing the *omcB*-pET21a plasmid were stored as glycerol stocks in a -74°C freezer.

The full length *omcC* gene (2307 bp) was also amplified and expressed as described for the *omcB* gene. The forward primer sequence was: GCTAGCATGAGTAGAAAAGTAACAAAGTAT and the reverse primer sequence was: AAGCTTCG-GACGGGTCGC. The *NheI* and *HindIII* restriction enzyme sites are underlined, respectively.

### Purification of recombinant OmcB

For over expression and purification of the recombinant OmcB protein, *E. coli* cells harboring the *omcB*-pET21a plasmid were inoculated into 500 mL of LB medium containing 100 μg/mL ampicillin and 35 μg/mL chloramphenicol and grown and induced as previously described. The cells were harvested by centrifugation at 7,311×g for 10 minutes at 4°C and stored at -74°C. Purification was via a procedure modified from that used by [66]. The cell pellet was resuspended in 0.4 volumes of 50 mM Tris-Cl, pH 8 with 2 mM EDTA and 10 mM DTT. Next, 0.01 volumes of 10 mM PMSF in 90% isopropanol, 10 mg/mL lysozyme and 1% Triton X-100 were added to the cell suspension. The cell suspension was incubated at 30°C for 30 minutes and the cells sonicated five times for 1 minute each time, on ice. The cell suspension was then centrifuged at 7,311×g for 20 minutes at 5°C. The pellet was stored at -20°C. The pellet was resuspended in just enough 50 mM Tris-Cl, pH 8 buffer with 8 M urea, 2 mM EDTA and 1 mM DTT to get the pellet into solution. A homogenizer was used to fully resuspend the pellet in the buffer.

The pellet solution was applied to a Ni-NTA column (Qiagen) equilibrated with the binding buffer (100 mM NaH<sub>2</sub>PO<sub>4</sub>, 10 mM Tris-Cl and 8 M urea, pH 8). The flow through fraction was collected and the column washed with 3 volumes of the wash buffer (100 mM NaH<sub>2</sub>PO<sub>4</sub>, 10 mM Tris-Cl and 8 M urea, pH 6.3). The wash fraction was collected and the OmcB protein that was bound to the column was eluted with 10 mL of elution buffer (100 mM NaH<sub>2</sub>PO<sub>4</sub>, 10 mM Tris-Cl, 8 M urea and 0.5 M imidazole, pH 8). All three fractions were then resolved on a 12% SDS-PAGE. Coomassie staining of the gel revealed that the eluted fraction consisted mostly of the OmcB protein. The eluted fraction was then diluted with distilled H<sub>2</sub>O (to dilute the 8 M urea) and concentrated in an Amicon stirred cell with a 10 kDa cutoff (Millipore) at 4°C to a volume of 1 mL. The concentrated, purified protein was dialyzed at 4°C in 5 mM NaH<sub>2</sub>PO<sub>4</sub> buffer, pH 7. One exchange of buffer was performed and the pure protein was stored at -20°C. Removal of the urea resulted in some precipitation of OmcB. The protein concentration was determined via the Lowry assay [67] with BSA as the standard.

### Peptides of acetate kinase for antibody preparation

Two peptides for labeling both acetate kinase isozymes were selected from the protein sequences using the hydropathicity plots program on [www.vivo.colostate.edu](http://www.vivo.colostate.edu) (Colorado State University).

The peptides selected, RRDVIEHASNGDHRC and CIEGLE-GIGIKLDRERNKGAM, are hydrophilic and putative antigenic regions of the protein, suitable for antibody production. The sequences were then compared to other protein sequences on the non-redundant protein database through NCBI Protein BLAST program. The peptides only matched acetate kinase in *G. sulfurreducens* PCA with the first peptide matching AckA-1 (GSU2707) and the second peptide matching AckA-1 and AckA-2 (GSU3448). The sequence of the second peptide matching AckA-2 was GIKLDRERN and the lysine residue was substituted with an arginine residue in AckA-2. A cysteine residue was placed at the amine terminus of the second peptide so that it could be linked to a carrier protein for antibody production. Both peptides were synthesized by the Penn State Hershey Macromolecular Core Facility.

### Antibody production

Purified OmcB protein and acetate kinase peptides were sent to Covance Custom Immunology Services Inc. (Princeton, NJ) as antigens for antibody preparation. Antibodies were made in New Zealand White rabbits. Antibodies to OmcB were affinity purified as previously described [68]. The affinity purified antibody was kept at  $-20^{\circ}\text{C}$ .

The acetate kinase peptides were covalently linked to a Sulfolink Coupling Resin (Pierce Biotechnology, Rockford, IL) at the cysteine residue and used to affinity purify the acetate kinase antibodies. The peptides were linked to the Sulfolink resin based on the manufacturer's instructions. The acetate kinase antibodies were purified based on the procedure described in [69]. The OmcB and acetate kinase pre-immune sera were purified using Protein A agarose resin (Sigma Aldrich) according to the manufacturer's procedure. All antibody concentrations were determined using the Bradford assay [70].

### Detection of OmcB and Acetate kinase

Proteins from *G. sulfurreducens* whole cells or from the total membrane (TM) were separated on a SDS-PAGE and transferred to nitrocellulose for Western blotting with a 1:100 dilution of anti-OmcB affinity-purified antibody or 1:1000 dilution of anti-acetate kinase affinity-purified antibody. The polyclonal OmcB antibody produced only one cross-reactive band when 10  $\mu\text{g}$  of *G. sulfurreducens* total membrane protein was analyzed. *E. coli* expressing either OmcB or OmcC, a slightly larger homolog of OmcB which has 73% amino acid identity, was also analyzed via Western blotting. While OmcB was easily detected with the OmcB antibody, ten times more protein had to be loaded for Western blots to reveal a faint band for OmcC. Densitometry of the Western blots with calibrated levels of protein indicated the OmcB antibody had over 30-fold higher affinity for OmcB compared to OmcC.

As acetate kinase was intended to act as a control for cytoplasmic antibody labeling, synthetic peptides were used to generate an antibody able to recognize both acetate kinase isozymes expressed by *G. sulfurreducens*. Western blots of cells detected both forms, at 47 kDa and 44 kDa, with the major band being the isozyme of greater molecular weight. Previous proteomic data also reported significantly higher abundance of this isozyme under all growth conditions [31].

OmcB and acetate kinase pre-immune sera were also incubated with membrane proteins and whole cells, respectively, and did not show a band corresponding to OmcB or acetate kinase under any conditions. These pre-immune sera were used as controls for nonspecific labeling of biofilms.

### Immunolocalization of OmcB and acetate kinase in biofilm

Each carbon-coated copper grid containing a *Geobacter* biofilm slice (spanning the whole biofilm, top to bottom) was allowed to incubate sample-side down on a drop of TBS (10 mM Tris-Cl, pH 8, 150 mM NaCl), for 1 minute. Each grid was then placed on a drop of 0.3% glycine in TBS for 5 minutes and then on a drop of 1% BSA in TBS for 30 minutes. After this blocking step, each grid was incubated on a drop of 1:50 dilution of OmcB antibody (0.6  $\mu\text{g}$  total protein) in 1% BSA in TBS or on a drop of 1:100 dilution of acetate kinase antibody (4  $\mu\text{g}$  total protein). Separate grids incubated on purified pre-immune serum for OmcB and acetate kinase were used as controls. The grids that were used in the OmcB immunolabeling experiment were incubated in the antibody or pre-immune serum for 10 hours at  $4^{\circ}\text{C}$ , based on preliminary immunolabeling experiments with the OmcB antibody that showed long incubations at low temperature increased labeling without increasing non-specific binding by pre-immune serum controls. The grids for acetate kinase were incubated in the antibody or pre-immune serum at room temperature for 1 hour.

Each grid was then washed by placing it on a drop of TBS for 3 minutes (3 times) and then on a drop of 1% BSA in TBS for 3 minutes (5 times) to block the biofilm before labeling with the secondary antibody. Each grid was then allowed to incubate on a drop of the secondary antibody: goat anti-rabbit IgG secondary antibody conjugated to 20 nm gold particles (BB International), which was prepared as a 1:100 dilution in 1% BSA and 0.1% cold fish gelatin in TBS. The secondary antibody labeling was carried out for 1 hour at room temperature. Each grid was washed by placing it on a drop of TBS as described above and then the biofilms were fixed by incubating them on a drop of 1% glutaraldehyde in TBS for 5 minutes. After this step, each grid was washed by placing it on a drop of water for 3 minutes (7 times) and then negatively stained on a drop of 2% uranyl acetate in water for 5 minutes in the dark. Finally, each grid was washed on a drop of water for 1 minute (5 times) and allowed to dry completely (at least 12 hours) before TEM imaging.

### TEM imaging and analysis of biofilms

Immunolabeled biofilms were visualized using a JEOL 1200 EX II transmission electron microscope (Pennsylvania State University, University Park) at 80 kV and a magnification of 10,000. A series of TEM images were reconstructed into continuous biofilm pictures using Adobe Photoshop CS2. The ImageJ software (NIH) was then used to take subsamples of each biofilm, representing 2  $\mu\text{m}$  increments from the electrode surface. For each antibody and analysis, three complete biofilms were reconstructed.

ImageJ was also used to measure cell area within each slice with the Measure feature. The cell area values obtained from ImageJ were converted to  $\mu\text{m}^2$  values by determining the length of the 1  $\mu\text{m}$  scale bar in the TEM micrographs. The number of gold particles present inside cells, and at the membrane was counted using the Cell Counter plugin of ImageJ.

### Supporting Information

**Figure S1 Representative raw image.** Raw data from one complete set of 13 high-resolution images spanning an entire biofilm. Slices were labeled with *anti*-OmcB antibodies post-slicing. From this raw data, trends in both cell density, OmcB labeling, and protein localization can be seen before images were analyzed further. After this reconstruction, digital images were separated into fields encompassing distances from the electrode

discussed in the text and figures, and relative cell volume and labeling measured. (TIF)

## Acknowledgments

Thank you to Gilbert Ahlstrand at the University of Minnesota for embedding biofilms for TEM, also Dr. Gang Ning and Missy Hazen of the Penn State Microscopy and Cytometry Facility (University Park, PA) for assistance with sample preparation for TEM. Thank you to Dr. Scott Geib and Dr. Ruth Nissly for suggestions on data analysis and Dr. Bruce Logan

## References

- Lovley D (2006) Dissimilatory Fe(III)- and Mn(IV)-reducing prokaryotes. In: Dworkin M, Falkow S, Rosenberg E, Schleifer K-H, Stackebrandt E, editors. *The Prokaryotes*. 3 ed. New York: Springer. pp. 635–658.
- Kasting JF, Siefert JL (2002) Life and the evolution of earth's atmosphere. *Science* 296: 1066–1068.
- Lovley DR (1991) Dissimilatory Fe(III) and Mn(IV) reduction. *Microbiol Rev* 55: 259–287.
- Lovley DR (1993) Anaerobes into heavy metal: dissimilatory metal reduction in anoxic environments. *Trends Ecol Evol* 8: 213–217.
- N'guessan AL, Vrionis HA, Resch CT, Long PE, Lovley DR (2008) Sustained removal of uranium from contaminated groundwater following stimulation of dissimilatory metal reduction. *Environ Sci Technol* 42: 2999–3004.
- Lovley DR (1995) Bioremediation of organic and metal contaminants with dissimilatory metal reduction. *J Industrial Microbiol* 14: 85–93.
- Caccavo F, Lonergan DJ, Lovley DR, Davis M, Stolz JF, et al. (1994) *Geobacter sulfurreducens* sp. nov., a hydrogen- and acetate-oxidizing dissimilatory metal-reducing microorganism. *Appl Environ Microbiol* 60: 3752–3759.
- Marsili E, Rollefson JB, Baron DB, Hozalski RM, Bond DR (2008) Microbial biofilm voltammetry: direct electrochemical characterization of catalytic electrode-attached biofilms. *Appl Environ Microbiol* 74: 7329–7337.
- Bond DR, Lovley DR (2003) Electricity production by *Geobacter sulfurreducens* attached to electrodes. *Appl Environ Microbiol* 69: 1548–1555.
- Ishii S, Watanabe K, Yabuki S, Logan BE, Sekiguchi Y (2008) Comparison of electrode reduction activities of *Geobacter sulfurreducens* and an enriched consortium in an air-cathode microbial fuel cell. *Appl Environ Microbiol* 74: 7348–7355.
- Marsili E, Sun J, Bond DR (2010) Voltammetry and growth physiology of *Geobacter sulfurreducens* biofilms as a function of growth stage and imposed electrode potential. *Electroanalysis* 22: 865–874.
- Snider RM, Strycharz-Glaven SM, Tsoi SD, Erickson JS, Tender LM (2012) Long-range electron transport in *Geobacter sulfurreducens* biofilms is redox gradient-driven. *Proc Natl Acad Sci USA* 109: 15467–15472.
- von Canstein H, Ogawa J, Shimizu S, Lloyd JR (2008) Secretion of flavins by *Shewanella* species and their role in extracellular electron transfer. *Appl Environ Microbiol* 74: 615–623.
- Covington ED, Gelbmann CB, Kotloski NJ, Gralnick JA (2010) An essential role for UshA in processing of extracellular flavin electron shuttles by *Shewanella oneidensis*. *Mol Micro* 78: 519–532.
- Brutinel ED, Gralnick JA (2012) Shuttling happens: soluble flavin mediators of extracellular electron transfer in *Shewanella*. *Appl Microbiol Biotechnol* 93: 41–48.
- Kotloski NJ, Gralnick JA (2013) Flavin electron shuttles dominate extracellular electron transfer by *Shewanella oneidensis*. *mBio* 4: e00553–12. doi: 10.1128/mBio.00553-12.
- Babauta JT, Nguyen HD, Harrington TD, Renslow R, Beyenal H (2012) pH, redox potential and local biofilm potential microenvironments within *Geobacter sulfurreducens* biofilms and their roles in electron transfer. *Biotechnol Bioeng* 109: 2651–2662.
- Liu Y, Kim H, Franklin RR, Bond DR (2011) Linking spectral and electrochemical analysis to monitor *c*-type cytochrome redox status in living *Geobacter sulfurreducens* biofilms. *ChemPhysChem* 12: 2235–2241.
- Liu Y, Bond DR (2012) Long-distance electron transfer by *G. sulfurreducens* biofilms results in accumulation of reduced *c*-type cytochromes. *ChemSusChem* 5: 1047–1053.
- Strycharz-Glaven SM, Snider RM, Guiseppi-Elie A, Tender LM (2011) On the electrical conductivity of microbial nanowires and biofilms. *Energy Environ Science* 4: 4366–4379.
- Robuschli L, Tomba JP, Schrott GD, Bonanni PS, Desimone PM, et al. (2013) Spectroscopic slicing to reveal internal redox gradients in electricity-producing biofilms. *Angewandte Chemie* 52: 925–928.
- Franks AE, Nevin KP, Jia HF, Izallalen M, Woodard TL, et al. (2009) Novel strategy for three-dimensional real-time imaging of microbial fuel cell communities: monitoring the inhibitory effects of proton accumulation within the anode biofilm. *Energy Environ Science* 2: 113–119.
- Torres CI, Kato Marcus A, Rittmann BE (2008) Proton transport inside the biofilm limits electrical current generation by anode-respiring bacteria. *Biotechnol Bioeng* 100: 872–881.
- Torres CI, Marcus AK, Lee H-S, Parameswaran P, Krajmalnik-Brown R, et al. (2010) A kinetic perspective on extracellular electron transfer by anode-respiring bacteria. *FEMS Microbiol Rev* 34: 3–17.
- Franks AE, Nevin KP, Glaven RH, Lovley DR (2010) Microtoming coupled to microarray analysis to evaluate the spatial metabolic status of *Geobacter sulfurreducens* biofilms. *ISME J* 4: 509–519.
- Inoue K, Leang C, Franks AE, Woodard TL, Nevin KP, et al. (2011) Specific localization of the *c*-type cytochrome OmcZ at the anode surface in current-producing biofilms of *Geobacter sulfurreducens*. *Environ Microbiol Reports* 3: 211–217.
- Franks AE, Glaven RH, Lovley DR (2012) Real-time spatial gene expression analysis within current-producing biofilms. *ChemSusChem* 5: 1092–1098.
- Leang C, Coppi MV, Lovley DR (2003) OmcB, a *c*-type polyheme cytochrome, involved in Fe(III) reduction in *Geobacter sulfurreducens*. *J Bacteriol* 185: 2096–2103.
- Leang C, Lovley DR (2005) Regulation of two highly similar genes, *omcB* and *omcC*, in a 10 kb chromosomal duplication in *Geobacter sulfurreducens*. *Microbiology* 151: 1761–1767.
- Chin KJ, Esteve-Nunez A, Leang C, Lovley DR (2004) Direct correlation between rates of anaerobic respiration and levels of mRNA for key respiratory genes in *Geobacter sulfurreducens*. *Appl Environ Microbiol* 70: 5183–5189.
- Ding YHR, Hixson KK, Giometti CS, Stanley A, Esteve-Nunez A, et al. (2006) The proteome of dissimilatory metal-reducing microorganism *Geobacter sulfurreducens* under various growth conditions. *Biochimica et Biophysica Acta* 1764: 1198–1206.
- Strycharz-Glaven SM, Tender LM (2012) Study of the mechanism of catalytic activity of *G. sulfurreducens* biofilm anodes during biofilm growth. *ChemSusChem* 5: 1106–1118.
- Rollefson JB, Levar CE, Bond DR (2009) Identification of genes involved in biofilm formation and respiration via mini-*Himar* transposon mutagenesis of *Geobacter sulfurreducens*. *J Bacteriol* 191: 4207–4217.
- Liu Y, Kim YS, Franklin R, Bond DR (2010) Gold line array electrodes increase substrate affinity and current density of electricity-producing *G. sulfurreducens* biofilms. *Energy Environ Sci* 3: 1782–1788.
- Pease LF, Elliott JT, Tsai DH, Zachariah MR, Tarlov MJ (2008) Determination of protein aggregation with differential mobility analysis: Application to IgG antibody. *Biotechnology and Bioengineering* 101: 1214–1222.
- Bond DR, Strycharz-Glaven SM, Tender LM, Torres CI (2012) On electron transport through *Geobacter* biofilms. *ChemSusChem* 5: 1099–1105.
- Torres CI, Lee H, Rittmann BE (2008) Carbonate species as OH<sup>-</sup> carriers for decreasing the pH gradient between cathode and anode in biological fuel cells. *Environ Sci Technol* 42: 8773–8777.
- Mehta T, Coppi MV, Childers SE, Lovley DR (2005) Outer membrane *c*-type cytochromes required for Fe(III) and Mn(IV) oxide reduction in *Geobacter sulfurreducens*. *Appl Environ Microbiol* 71: 8634–8641.
- Shelobolina ES, Coppi MV, Korenevsky AA, DiDonato LN, Sullivan SA, et al. (2007) Importance of *c*-type cytochromes for U(VI) reduction by *Geobacter sulfurreducens*. *BMC Microbiology* 7:16. doi:10.1186/1471-2180-7-16.
- Kim BC, Leang C, Ding YH, Glaven RH, Coppi MV, et al. (2005) OmcF, a putative *c*-type monoheme outer membrane cytochrome required for the expression of other outer membrane cytochromes in *Geobacter sulfurreducens*. *J Bacteriol* 187: 4505–4513.
- Lloyd JR, Leang C, Hodges Myerson AL, Coppi MV, Cuiño S, et al. (2003) Biochemical and genetic characterization of PpcA, a periplasmic *c*-type cytochrome in *Geobacter sulfurreducens*. *Biochemical J* 369: 153–161.
- Ding YH, Hixson KK, Akujkar MA, Lipton MS, Smith RD, et al. (2008) Proteome of *Geobacter sulfurreducens* grown with Fe(III) oxide or Fe(III) citrate as the electron acceptor. *Biochimica et Biophysica Acta* 1784: 1935–1941.
- Inoue K, Qian X, Morgado L, Kim B-C, Mester T, et al. (2010) Purification and characterization of OmcZ, an outer-surface, octaheme *c*-type cytochrome essential for optimal current production by *Geobacter sulfurreducens*. *Appl Environ Microbiol* 76: 3999–4007.
- Magnuson TS, Isoyama N, Hodges-Myerson AL, Davidson G, Maroney MJ, et al. (2001) Isolation, characterization and gene sequence analysis of a membrane-associated 89 kDa Fe(III) reducing cytochrome *c* from *Geobacter sulfurreducens*. *Biochemical J* 359: 147–152.

45. Magnuson TS, Hodges-Myerson AL, Lovley DR (2000) Characterization of a membrane-bound NADH-dependent Fe<sup>3+</sup> reductase from the dissimilatory Fe<sup>3+</sup>-reducing bacterium *Geobacter sulfurreducens*. FEMS Microbiol Lett 185: 205–211.
46. Qian X, Reguera G, Mester T, Lovley DR (2007) Evidence that OmcB and OmpB of *Geobacter sulfurreducens* are outer membrane surface proteins. FEMS Microbiol Lett 277: 21–27.
47. Kim BC, Qian XL, Ching LA, Coppi MV, Lovley DR (2006) Two putative *c*-type multiheme cytochromes required for the expression of OmcB, an outer membrane protein essential for optimal Fe(III) reduction in *Geobacter sulfurreducens*. J Bacteriol 188: 3138–3142.
48. Kim BC, Lovley DR (2008) Investigation of direct vs. indirect involvement of the *c*-type cytochrome MacA in Fe(III) reduction by *Geobacter sulfurreducens*. FEMS Microbiol Lett 286: 39–44.
49. Seidel J, Hoffmann M, Ellis KE, Seidel A, Spatzal T, et al. (2012) MacA is a second cytochrome *c* peroxidase of *Geobacter sulfurreducens*. Biochemistry 51: 2747–2756.
50. Kim BC, Postier BL, DiDonato RJ, Chaudhuri SK, Nevin KP, et al. (2008) Insights into genes involved in electricity generation in *Geobacter sulfurreducens* via whole genome microarray analysis of the OmcF-deficient mutant. Bioelectrochemistry 73: 70–75.
51. Butler JE, Kaufmann F, Coppi MV, Núñez C, Lovley DR (2004) MacA, a diheme *c*-type cytochrome involved in Fe(III) reduction by *Geobacter sulfurreducens*. J Bacteriol 186: 4042–4045.
52. Nevin KP, Kim BC, Glaven RH, Johnson JP, Woodard TL, et al. (2009) Anode biofilm transcriptomics reveals outer surface components essential for high density current production in *Geobacter sulfurreducens* fuel cells. PLoS ONE 4: e5628. doi:10.1371/journal.pone.0005628.
53. Holmes DE, Chaudhuri SK, Nevin KP, Mehta T, Methé BA, et al. (2006) Microarray and genetic analysis of electron transfer to electrodes in *Geobacter sulfurreducens*. Environ Microbiol 8: 1805–1815.
54. Itoh Y, Rice JD, Goller C, Pannuri A, Taylor J, et al. (2008) Roles of *pgaABCD* genes in synthesis, modification, and export of the *Escherichia coli* biofilm adhesin poly-β-1,6-N-acetyl-d-glucosamine. J Bacteriol 190: 3670–3680.
55. Li Z, Clarke AJ, Beveridge TJ (1996) A major autolysin of *Pseudomonas aeruginosa*: subcellular distribution, potential role in cell growth and division and secretion in surface membrane vesicles. J Bacteriol 178: 2479–2488.
56. Garduño RA, Faulkner G, Trevors MA, Vats N, Hoffman PS (1998) Immunolocalization of Hsp60 in *Legionella pneumophila*. J Bacteriol 180: 505–513.
57. Martínez RM, Dharmasena MN, Kirn TJ, Taylor RK (2009) Characterization of two outer membrane proteins, FlgO and FlgP, that influence *Vibrio cholerae* motility. J Bacteriol 191: 5669–5679.
58. Graham LL, Beveridge TJ (1990) Effect of chemical fixatives on accurate preservation of *Escherichia coli* and *Bacillus subtilis* structure in cells prepared by freeze-substitution. J Bacteriol 172: 2150–2159.
59. Yan B, Nunez C, Ueki T, Esteve-Nunez A, Puljic M, et al. (2006) Computational prediction of RpoS and RpoD regulatory sites in *Geobacter sulfurreducens* using sequence and gene expression information. Gene 384: 73–95.
60. Nunez C, Esteve-Nunez A, Giometti C, Tollaksen S, Khare T, et al. (2006) DNA microarray and proteomic analyses of the RpoS regulon in *Geobacter sulfurreducens*. J Bacteriol 188: 2792–2800.
61. Nunez C, Adams L, Childers S, Lovley DR (2004) The RpoS sigma factor in the dissimilatory Fe(III)-reducing bacterium *Geobacter sulfurreducens*. J Bacteriol 186: 5543–5546.
62. DiDonato LN, Sullivan SA, Methé BA, Nevin KP, England R, et al. (2006) Role of Rel<sub>Gsu</sub> in stress response and Fe(III) reduction in *Geobacter sulfurreducens*. J Bacteriol 188: 8469–8478.
63. Krushkal J, Yan B, DiDonato LN, Puljic M, Nevin KP, et al. (2007) Genome-wide expression profiling in *Geobacter sulfurreducens*: identification of Fur and RpoS transcription regulatory sites in a *relGsu* mutant. Funct Int Genomics 7: 229–255.
64. Yang TH, Coppi MV, Lovley DR, Sun J (2010) Metabolic response of *Geobacter sulfurreducens* towards electron donor/acceptor variation. Microbial Cell Fact 9:90. doi:10.1186/1475-2859-9-90.
65. Arslan E, Schulz H, Zufferey R, Künzler P, Thöny-Meyer L (1998) Overproduction of the *Bradyrhizobium japonicum* *c*-type cytochrome subunits of the *cbh3* oxidase in *Escherichia coli*. Biochem Biophys Res Comm 251: 744–747.
66. Whitwam RE, Gazarian IG, Tien M (1995) Expression of fungal Mn peroxidase in *E. coli* and refolding to yield active enzyme. Biochem Biophys Res Comm 216: 1013–1017.
67. Lowry OH, Rosebrough NJ, Farr AL, Randal RJ (1951) Protein measurement with the Folin phenol reagent. J Biol Chem 193: 265–275.
68. Ross DE, Ruebush SS, Brantley SL, Hartshorne RS, Clarke TA, et al. (2007) Characterization of protein-protein interactions involved in iron reduction by *Shewanella oneidensis* MR-1. Appl Environ Microbiol 73: 5797–5808.
69. Rollefson JB, Stephen CS, Tien M, Bond DR (2011) Identification of an extracellular polysaccharide network essential for cytochrome anchoring and biofilm formation in *Geobacter sulfurreducens*. J Bacteriol 193: 1023–1033.
70. Bradford MM (1976) A rapid and sensitive method for the quantitation of microgram quantities of protein utilizing the principle of protein-dye binding. Analytical Biochemistry 72: 248–254.